

# Learning Multi-Modal Nonlinear Embeddings: Performance Bounds and an Algorithm

Semih Kaya and Elif Vural

**Abstract**—While many approaches exist in the literature to learn representations for data collections in multiple modalities, the generalizability of the learnt representations to previously unseen data is a largely overlooked subject. In this work, we first present a theoretical analysis of learning multi-modal nonlinear embeddings in a supervised setting. Our performance bounds indicate that for successful generalization in multi-modal classification and retrieval problems, the regularity of the interpolation functions extending the embedding to the whole data space is as important as the between-class separation and cross-modal alignment criteria. We then propose a multi-modal nonlinear representation learning algorithm that is motivated by these theoretical findings, where the embeddings of the training samples are optimized jointly with the Lipschitz regularity of the interpolators. Experimental comparison to recent multi-modal and single-modal learning algorithms suggests that the proposed method yields promising performance in multi-modal image classification and cross-modal image-text retrieval applications.

**Index Terms**—Multi-modal learning, multi-view learning, cross-modal retrieval, nonlinear embeddings, supervised embeddings, RBF interpolators.

## I. INTRODUCTION

WITH the increasing accessibility of data acquisition and storing technologies, the need for successfully analyzing and interpreting multi-modal data collections has become more important. Many applications involve the requirement or analysis of data collections available in multiple modalities. In some problems, the purpose is to fuse the information in different modalities to attain higher detection or classification accuracy than in a single-modality. For instance, the integration of multi-modal medical data such as patient information, MRI scans and ECG recordings may lead to more accurate clinical decisions. Similarly, an image sample and a text sample extracted from the same web page can be seen as the observations of the same data in two different modalities, which can be used together for the categorization of the web page. Meanwhile, some other applications require the retrieval of data samples in a certain modality while relevant query samples are provided in another modality. For instance, in an image-text cross-modal retrieval problem, a text sample may be provided as query and one might be interested in retrieving image samples belonging to the same category as the query text sample, as in web image search applications. In this paper, we study the problem of learning supervised nonlinear representations for multi-modal classification and cross-modal retrieval applications.

Multi-modal learning algorithms often rely on computing joint representations for multi-modal data in a common domain, where the main challenge is to efficiently align data samples from different modalities without damaging the inherent geometry of the individual modalities. The main approaches in the literature are as follows. Subspace learning methods such as CCA [1] align different modalities via linear projections or transformations. Supervised variants of such linear embedding methods aim to enhance the separation between different data classes [2], [3] in addition to the alignment of different modalities. However, such linear embedding methods have limitations in challenging data sets where different modalities are weakly linked. In particular, when the data from different modalities have significantly dissimilar geometric structures, linear methods may fall short of learning effective joint representations since they are mostly restricted by the original geometry of the individual modalities.

Kernel extensions of linear methods provide nonlinear representations that may improve some of these shortcomings [1]; however, the resulting algorithms might still lack in flexibility in certain problems. In particular, the suitability of the selected kernel type might vary largely depending on the structure of the data set and there is often no guarantee that the learnt embedding will perform well on the test data at hand.

In the recent years, impressive performance has been attained in retrieval and classification problems with deep learning algorithms based on cross-modal CNNs and autoencoders [4], [5], [6]. While such methods can compute effective and powerful nonlinear representations, they typically require much larger data sets compared to subspace methods or their nonlinear kernel extensions, and their training complexity is significantly higher.

While the aforementioned multi-modal learning approaches might be preferable to each other depending on the setting, their capacity to generalize to novel test samples is a questionable issue in general. A multi-modal learning method may yield promising performance figures on training data, e.g., it may perfectly align different modalities and separate training samples from different classes, while its performance may be much lower on previously unseen test data. In particular, due to the limited capacity of the model they learn, linear subspace methods may be expected to have relatively close accuracy on training and test data. On the other hand, more sophisticated methods such as deep learning algorithms computing complex and rich models may suffer from overfitting if the amount of training data is insufficient. Although the learnt model fits to the characteristics of the training data very well, it might fail to generalize to previously unseen test data.

S. Kaya and E. Vural are with the Department of Electrical and Electronics Engineering, METU, Ankara.  
E-mail: kaya.semih@metu.edu.tr, velif@metu.edu.tr

In fact, the theoretical characterization of the generalization capability of multi-modal learning algorithms is a largely overlooked problem in the literature, despite its importance. The previous study [7] proposes generalization bounds on the performance of supervised nonlinear embedding algorithms; however, it treats the problem in a single modality. To the best of our knowledge, a mathematically rigorous study of the performance of supervised multi-modal embedding algorithms has not been proposed so far.

In this paper, we consider the problem of learning supervised nonlinear embeddings for multi-modal classification and cross-modal retrieval applications that can generalize well to new test data. Our main purpose in preferring a nonlinear embedding approach as opposed to linear subspace methods is to achieve a relatively high model capacity that can adapt to challenging data geometries. On the other hand, we adhere to a shallow data representation model consisting of a single-stage embedding as opposed to deep methods, in order to achieve applicability to settings with restricted availability of training data or limited computation budget. Our effort hence seeks a balance between the ease of training (which linear subspace methods have) and the richness and flexibility of nonlinear representation models (which deep learning methods have), while ensuring good generalizability to new test data.

Our study has two main contributions. We first propose a theoretical analysis of the problem of learning supervised multi-modal embeddings. We provide an extension of the results in [7] to the multi-modal setting. We consider a nonlinear embedding model where the training samples from different modalities are jointly mapped to a common lower-dimensional domain. The extension of the embedding to new test samples is achieved via Lipschitz-continuous interpolation functions that generalize the pointwise embeddings to the data space of each modality. Our theoretical bounds suggest that in order to attain good generalization performance in classification and retrieval applications, the multi-modal embedding of training samples should satisfy three conditions: (1) Different modalities should be aligned sufficiently well; (2) Different classes should be sufficiently well-separated from each other; (3) The geometric structure of each modality (captured through nearest neighborhoods) should be preserved. Then, under these conditions, our theoretical analysis shows that the embedding generalizes well to test data, provided that the Lipschitz constants of the interpolation functions are sufficiently low. This points to an important trade-off in learning nonlinear embeddings: Multi-modal methods may fail to generalize to test data if the nonlinear interpolation functions are too irregular, even if the embeddings of training samples exhibit good cross-modal alignment and between-class separation properties.

Our next contribution is to propose a new supervised nonlinear multi-modal learning algorithm. Motivated by the above theoretical findings, we formulate an optimization problem where a cross-modal alignment term and a between-class separation term for the embeddings of the training samples are jointly optimized with the Lipschitz constants of the interpolation functions that generalize the embeddings to the ambient space of each modality. The resulting objective function is minimized with an iterative optimization procedure, where

the nonlinear embedding coordinates are learnt jointly with the Lipschitz-continuous interpolator parameters. Compared to existing approaches, our method has the advantage of providing more flexible representations than subspace methods thanks to the employed nonlinear models, while it entails a much more lightweight training phase compared to more elaborate approaches such as deep learning methods. We test the proposed algorithm in multi-view image classification and image-text cross-modal retrieval applications. Experimental results show that the proposed method yields quite satisfactory performance in comparison with recent multi-modal learning approaches.

The rest of the paper is organized as follows. In Section II, we overview the related literature. In Section III, we present a theoretical analysis of the multi-modal representation learning problem. In Section IV, we propose a supervised nonlinear multi-modal representation learning algorithm that is motivated by the theoretical findings of Section III. In Section V, we experimentally evaluate the performance of the proposed method, and in Section VI, we conclude.

## II. RELATED WORK

The multi-modal (multi-view) learning approaches in the literature can be mainly grouped as co-training methods, multiple kernel learning algorithms, subspace learning-based approaches and deep learning methods. Co-training methods learn separate models in different modalities by encouraging their predictions to be similar [8]. The study in [9] improves the co-training algorithm using Expectation Maximization (EM) to assign probabilistic labels to unlabeled samples, where each modality classifier iteratively uses the probabilities of class labels. A probabilistic model for Support Vector Machine (SVM) is constructed in [10] based on the Co-EM approach. There also exist co-regression algorithms employing the co-training idea. A regression algorithm that uses two  $k$ -NN regressors is presented to learn appropriate labels for unlabeled samples in [11]. The co-training technique is also used in graph-based methods such as [12], where a Gaussian process model is used on an undirected Bayesian graph representation for all modalities. Co-training algorithms have been applied to the analysis of multi-modal data sets in various applications [13], [14], [15].

Subspace learning methods are based on computing linear projections or transformations that suitably align samples from different modalities. The well-known unsupervised subspace learning algorithm CCA (Canonical Correlation Analysis) maximizes the correlation between different modalities [1]. Alternative versions of CCA such as cluster CCA [16], multi-label CCA [17] and three-view CCA [18] have been proposed to improve the performance of CCA in various supervised tasks, all of which employ linear projections. In the recent years, many supervised subspace methods have been proposed, which aim to enhance the between-class separation and cross-modal alignment when learning linear projections of data. The GMLDA (Generalized Multiview Analysis) method proposes a multi-modal extension of the LDA algorithm within this framework [2]. The JFSSL (Joint Feature Selection and

Subspace Learning) method additionally uses a joint graphical model for calculating projections with relevant and irrelevant features [3]. Some other subspace learning methods propose solutions based on the metric learning [19] and matrix factorization [20] ideas.

Subspace learning methods have the advantage of involving relatively simple models; however, their performance may be poor in difficult data geometries where the distributions of the modalities are significantly different. Nonlinear methods offer more flexible representations in such cases. Nonlinear representations may follow from the kernel extensions of linear subspace methods. For instance, a nonlinear kernel extension of CCA (called Kernel CCA) can be found in [1] and [21]. Some other methods are based on combining kernels in different modalities. Convex combinations of multiple Laplacian kernels are learnt in [22], while the power mean of the kernels of multilayer graphs is used in semi-supervised learning in [23]. The problem of learning multiple kernels has also been explored in [24], [25], [26], [27], [28]. Unlike kernel methods, some multi-view algorithms compute nonlinear embedding coordinates in a non-parametric manner. The multi-view learning algorithm [29] finds a nonlinear low-dimensional representation for multi-modal data based on spectral embeddings. The graph-based multi-modal clustering approach in [30] computes a nonlinear embedding while jointly estimating a clustering of the multi-view data.

With the evolution of computation techniques in the recent years, many deep learning methods have been proposed for processing large multi-modal data sets. Deep multi-view autoencoders have been proposed in [4], [6], [31] for learning a shared representation across different data modalities. The method in [32] learns cross-weights between the different modality layers of a stacked denoising autoencoder structure. Convolutional neural network structures are also widely used for alignment in multi-modal applications, where the visual modality features obtained with CNNs are combined with features of other modalities [5], [33], [34]. The work in [35] proposes to train a separate classifier for each image modality using features generated by deep CNNs and then combine the classifier outputs of different views. GAN-type architectures are also used for adversarially training feature generators and domain discriminators across different modalities or domains [36]. The method in [37] proposes to learn a common latent representation for different modalities via a deep matrix factorization scheme.

Finally, some other previous works related to our study are the following. The theoretical analysis in [7] provides performance bounds for supervised nonlinear embeddings in a single modality. The idea in [7] is developed in this paper to perform a theoretical analysis for multi-modal embeddings. The previous work [38] proposes a supervised nonlinear dimensionality reduction algorithm via smooth representations like in our work; however, it treats the embedding problem in a single modality. Lastly, a preliminary version of our work was presented in [39]. The current paper builds on [39] by including a theoretical analysis of the multi-modal learning problem and significantly extending the experimental results.

### III. PERFORMANCE BOUNDS FOR MULTI-MODAL LEARNING WITH SUPERVISED EMBEDDINGS

In this section, we first describe the multi-modal representation learning setting considered in this study and then present a theoretical analysis of multi-modal classification and retrieval with supervised embeddings.

#### A. Notation and Setting

We consider a setting with  $M$  data classes and  $V$  modalities (also called *views*) such that a data sample  $x$  has an observation  $x^{(v)}$  in each modality (or view)  $v = 1, \dots, V$ . Let the data samples from each class  $m = 1, \dots, M$  in each modality  $v = 1, \dots, V$  be drawn from a probability measure  $\nu_m^{(v)}$  on a Hilbert space  $H^{(v)}$ . We assume that the probability measure  $\nu_m^{(v)}$  has a bounded support  $\mathcal{M}_m^{(v)} \subset H^{(v)}$  for each  $v$ , and that the probability measures  $\{\nu_m^{(v)}\}$  in different modalities  $v$  are independent for each class  $m$ .

Let  $\mathcal{X} = \{x_i\}$  be a set of training samples such that each  $i$ -th training sample  $x_i$  belongs to one of the classes  $m = 1, \dots, M$ . In each modality  $v$ , the observations of the training samples  $\{x_i^{(v)}\}$  from each class  $m$  are independent and identically distributed, drawn from the probability measure  $\nu_m^{(v)}$ . In this paper, we study a setting where the training samples from all modalities are embedded as  $\mathcal{Y} = \{y_i^{(v)}\}$  into a common Euclidean domain  $\mathbb{R}^d$ , such that each training sample  $x_i^{(v)} \in H^{(v)}$  from modality  $v$  is mapped to a vector  $y_i^{(v)} \in \mathbb{R}^d$ . Although we do not impose any conditions on the dimension  $d$  of the embedding,  $d$  is typically small in many methods.

Focusing mainly on a scenario where the embedding is nonlinear in this work, we assume that the embedding of the training samples is extended to the whole data space through interpolation functions  $f^{(v)} : H^{(v)} \rightarrow \mathbb{R}^d$ , for  $v = 1, \dots, V$ , such that each training sample in a modality  $v$  is mapped to its embedding as  $f^{(v)}(x_i^{(v)}) = y_i^{(v)}$ . We characterize the regularity of the interpolation functions  $f^{(v)}$  with their Lipschitz continuity, which is defined as follows.

**Definition 1.** A function  $f : H \rightarrow \mathbb{R}^d$  defined on a Hilbert space  $H$  is Lipschitz continuous with constant  $L > 0$  if for any  $x_1, x_2 \in H$ , the function satisfies  $\|f(x_1) - f(x_2)\| \leq L \|x_1 - x_2\|$ .

The notation  $\|\cdot\|$  will denote the usual norm in the space of interest (e.g.  $L^2$ -norm, or  $\ell^2$ -norm), unless stated otherwise. Now, for each modality  $v$ , let  $B_\delta(x^{(v)}) \subset H^{(v)}$  be an open ball of radius  $\delta$  around the point  $x^{(v)}$

$$B_\delta(x^{(v)}) = \{z^{(v)} \in H^{(v)} : \|x^{(v)} - z^{(v)}\| < \delta\}.$$

Then, for each class  $m$ , we define a parameter  $\eta_{m,\delta}$ , which is a lower bound on the measure of the open ball  $B_\delta(x^{(v)})$  around any point from class  $m$  in any modality

$$\eta_{m,\delta} := \min_{v=1,\dots,V} \inf_{x^{(v)} \in \mathcal{M}_m^{(v)}} \nu_m^{(v)}(B_\delta(x^{(v)})).$$

In the following,  $C(\cdot)$  denotes the class label of a sample,  $|\cdot|$  refers to the cardinality of a set, the notation  $z \sim \nu$  means that the sample  $z$  is drawn from the distribution  $\nu$ ,  $P(\cdot)$  denotes

the probability of an event, and  $\|\cdot\|_F$  denotes the Frobenius norm. The notation  $\text{tr}(\cdot)$  stands for the trace of a matrix, and  $(\cdot)_{ij}$  indicates the entry of a matrix in the  $i$ -th row and the  $j$ -th column.

### B. Theoretical Analysis of Classification and Retrieval Performance

We now present performance bounds for the multi-modal classification problem and the cross-modal retrieval problem.

**1) Multi-Modal Classification Performance:** Let  $x$  be a test sample with an observation  $x^{(v)}$  available in a specific modality  $v$ . Denoting the true class of  $x$  by  $m$ , we assume that the observation  $x^{(v)}$  of the test sample is drawn from the probability measure  $\nu_m^{(v)}$  independently of the training samples.

We consider a classification setting where the class label of  $x^{(v)}$  is estimated by first embedding  $x^{(v)}$  into  $\mathbb{R}^d$  as  $f^{(v)}(x^{(v)})$  through the interpolator  $f^{(v)}$  learnt using the training samples. Then the estimate  $\hat{C}(x)$  of the class label  $C(x)$  of  $x$  is found via nearest-neighbor classification in  $\mathbb{R}^d$  over the embeddings  $y_i^{(u)}$  of the training samples  $x_i^{(u)}$  from all modalities  $u = 1, \dots, V$ . Hence, the class label of the test sample  $x$  is estimated as  $\hat{C}(x) = C(x_{i^*})$ , where <sup>1</sup>

$$i^* = \arg \min_i \min_{u=1, \dots, V} \|y_i^{(u)} - f^{(v)}(x^{(v)})\|. \quad (1)$$

Before stating our main result, we first present the following lemma.

**Lemma 1.** *Let the training sample set  $\mathcal{X}$  contain at least  $N_m$  training samples  $\{x_i\}_{i=1}^{N_m}$  from class  $m$ , whose observations  $\{x_i^{(u)}\}$  with  $x_i^{(u)} \sim \nu_m^{(u)}$  are available in all modalities  $u = 1, \dots, V$ . Assume that the interpolation function  $f^{(u)} : H^{(u)} \rightarrow \mathbb{R}^d$  in each modality  $u$  is Lipschitz continuous with constant  $L$ .*

*Let  $x$  be a test sample from class  $m$  with an observation  $x^{(v)}$  given in modality  $v$ , drawn with respect to the probability measure  $\nu_m^{(v)}$  independently of the training samples. Let  $x^{(u)}$  be the observation of the same sample  $x$  in an arbitrary modality  $u$ , which need not be available to the learning algorithm. For an arbitrary modality  $u \in \{1, \dots, V\}$ , define  $A^{(u)}$  as the set of the training samples from class  $m$  within a  $\delta$ -neighborhood of  $x^{(u)}$  in  $H^{(u)}$*

$$A^{(u)} = \{x_i^{(u)} : x_i \in \mathcal{X}, C(x_i) = m, x_i^{(u)} \in B_\delta(x^{(u)})\}.$$

*Assume that for some  $Q \geq 1$  and  $\delta > 0$ , the number of training samples from class  $m$  satisfies*

$$N_m > \frac{Q}{\eta_{m,\delta}}.$$

*Then for any  $\epsilon > 0$ , with probability at least*

$$1 - \exp\left(-\frac{2(N_m \eta_{m,\delta} - Q)^2}{N_m}\right) - 2d \exp\left(-\frac{Q\epsilon^2}{2L^2\delta^2}\right) - (1 - \eta_{m,\delta})^Q,$$

<sup>1</sup>We adopt the notation  $C(x)$  instead of  $C(x^{(v)})$  for class labels as the observation  $x^{(v)}$  of a sample  $x$  in any modality  $v$  has the same class label.

*the set  $A^{(u)}$  contains at least  $Q$  samples, the distance between  $f^{(u)}(x^{(u)})$  and the sample mean of the embeddings of its neighboring training samples is bounded as*

$$\left\| f^{(u)}(x^{(u)}) - \frac{1}{|A^{(u)}|} \sum_{x_i^{(u)} \in A^{(u)}} f^{(u)}(x_i^{(u)}) \right\| \leq L\delta + \sqrt{d}\epsilon, \quad (2)$$

*and also there is at least one  $x_i^{(u)} \in A^{(u)}$  such that its observation  $x_i^{(v)}$  in modality  $v$  satisfies  $\|x_i^{(v)} - x^{(v)}\| \leq \delta$ .*

Lemma 1 is proved in the Appendix. The purpose of Lemma 1 is to see how much the embedding of a test sample through a Lipschitz-continuous interpolator is expected to deviate from the average embedding of the training samples surrounding it. Lemma 1 provides a probabilistic upper bound on this deviation, which is used in Theorems 1 and 2 for bounding the classification and retrieval errors. Note that the classification algorithm knows the observation  $x^{(v)}$  of the test sample  $x$  only in modality  $v$ , and classifies it through its embedding  $f^{(v)}(x^{(v)})$  with respect to the rule in (1). The entity  $x^{(u)}$  in the lemma denotes a hypothetical observation of  $x$  in an arbitrary modality  $u$ . Although we conceptually refer to  $x^{(u)}$  in the derivations, it is not known to the classification algorithm in practice (unless  $u = v$ ).

In the following theorem, we present our main result for multi-modal classification with supervised embeddings.

**Theorem 1.** *Let the training sample set  $\mathcal{X}$  contain at least  $N_m$  training samples  $\{x_i\}_{i=1}^{N_m}$  from class  $m$ , whose observations  $\{x_i^{(u)}\}$  with  $x_i^{(u)} \sim \nu_m^{(u)}$  are available in all modalities  $u = 1, \dots, V$ . Let  $\mathcal{Y}$  be an embedding of  $\mathcal{X}$  in  $\mathbb{R}^d$  with the following properties*

- (P1)  $\|y_i^{(v)} - y_i^{(u)}\| \leq \eta$  for all training samples  $x_i$  and for all  $v, u \in \{1, \dots, V\}$
- (P2)  $\|y_i^{(u)} - y_j^{(u)}\| \leq R_\delta$  for all  $u \in \{1, \dots, V\}$ , if  $\|x_i^{(u)} - x_j^{(u)}\| \leq 2\delta$  and  $C(x_i) = C(x_j)$
- (P3)  $\|y_i^{(v)} - y_j^{(u)}\| > \gamma$  for all  $v, u \in \{1, \dots, V\}$  if  $C(x_i) \neq C(x_j)$

*where  $\eta$  and  $\gamma$  are some constants and  $R_\delta$  is a  $\delta$ -dependent constant. Assume that the interpolation function  $f^{(u)} : H^{(u)} \rightarrow \mathbb{R}^d$  in each modality  $u$  is a Lipschitz continuous function with constant  $L$  such that for some parameters  $\epsilon > 0$  and  $\delta > 0$ , the following inequality is satisfied*

$$6L\delta + 2\sqrt{d}\epsilon + 2R_\delta + 2\eta \leq \gamma. \quad (3)$$

*Then for some  $Q \geq 1$ , if the number of training samples is such that*

$$N_m > \frac{Q}{\eta_{m,\delta}}, \quad (4)$$

*the probability of correctly classifying a test sample  $x$  from class  $m$  observed as  $x^{(v)}$  in modality  $v$  via the nearest*

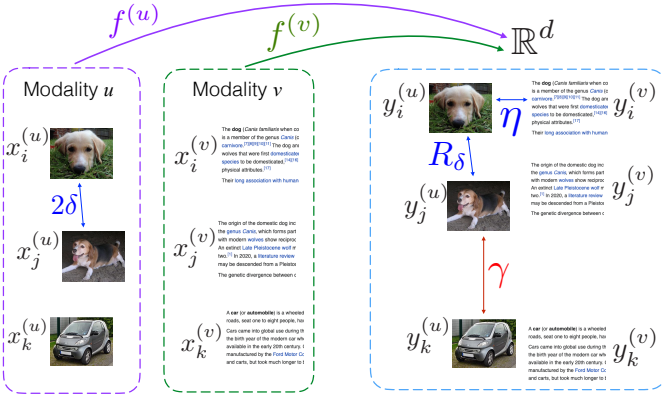


Fig. 1. Illustration of the studied multi-modal embedding setting. Modalities  $u$  (image) and  $v$  (text) are mapped to the common domain  $\mathbb{R}^d$  via interpolators  $f^{(u)}$  and  $f^{(v)}$ . The parameters  $\eta$ ,  $R_\delta$ , and  $\gamma$  respectively measure the alignment between different modalities, the within-class compactness, and the separation between different classes. (Images: wikipedia.org)

neighbor classification rule in (1) is lower bounded as

$$P\left(\hat{C}(x) = m\right) \geq 1 - \left[ \exp\left(-\frac{2(N_m \eta_{m,\delta} - Q)^2}{N_m}\right) + 2d \exp\left(-\frac{Q\epsilon^2}{2L^2\delta^2}\right) + (1 - \eta_{m,\delta})^Q \right]^V. \quad (5)$$

The proof of Theorem 1 is given in the Appendix. The theorem intuitively states the following: First, (P1), (P2), and (P3) define the properties that the embedding should have, which are illustrated in Figure 1. (P1) requires the observations  $x_i^{(v)}$ ,  $x_i^{(u)}$  of the same training sample  $x_i$  in two different modalities to be mapped to nearby points in the common domain  $\mathbb{R}^d$  of embedding, so that the distance between their embeddings does not exceed some threshold  $\eta > 0$ . This property imposes that different modalities be well aligned through the learnt embedding. The property (P2) indicates that two nearby samples from the same modality and the same class should be mapped to nearby points, so that a distance of  $2\delta$  in the original domain is mapped to a distance of at most  $R_\delta$  in the domain of embedding, where  $R_\delta$  is a constant depending on  $\delta$ . This can be seen as a condition for the preservation of the local geometry of each modality within the same class. Lastly, the property (P3) imposes samples from different classes to be separated by a distance of at least  $\gamma$  in the domain of embedding, regardless of their modality. Here, the parameter  $\gamma > 0$  can be seen as a separation margin between different classes in the learnt embedding.

If the embedding of the training samples has these properties, supposing that the condition in (3) is satisfied, Theorem 1 guarantees that the probability of correctly classifying a test sample from some class  $m$  approaches 1 at an exponential rate as the number of training samples  $N_m$  from that class increases. This can be verified by observing that  $N_m$  should be chosen proportionally to the parameter  $Q$  as seen in (4), in which case the correct classification probability in (5) improves at rate  $1 - e^{-O(VN_m)}$ . Here, an important observation is that as the number of modalities  $V$  increases, the

correct classification probability improves at an exponential rate. This confirms that the multi-modal learning algorithm can successfully fuse the information obtained from different modalities for improving the classification performance.

Finally, a crucial implication of Theorem 1 is that the condition in (3) must be satisfied in order to achieve high classification accuracy. The condition (3) is quite central to our study and it will be of importance when proposing an algorithm in Section IV. It states that a certain compromise must be sought between the Lipschitz regularity of the interpolator and the separation between different classes: When learning nonlinear embeddings, the separation  $\gamma$  between training samples from different classes should be adjusted in a way to allow the existence of a sufficiently regular interpolator, so that  $L$  remains sufficiently small. While an embedding with a too small  $\gamma$  value would fail to satisfy the condition (3), increasing  $\gamma$  too much would result in a highly irregular warping of the training samples, which typically leads to an increase in the magnitude of the interpolator parameters. This results in an interpolator with poor Lipschitz regularity with a large  $L$  value where the condition (3) would fail again. Hence, the condition (3) points to how the separation margin and the interpolator regularity should be jointly taken into account when learning an embedding with good generalization properties.

**2) Cross-Modal Retrieval Performance:** Next, we analyze the performance of cross-modal retrieval via supervised embeddings. Given the multi-modal data set  $\mathcal{X} = \{x_i\}$ , where each data sample  $x_i$  belongs to one of the classes  $m = 1, \dots, M$ , we formally define the retrieval problem as follows. Let  $x^{(v)}$  be a query test sample observed in modality  $v$ . We study a cross-modal retrieval setting where the purpose is to retrieve samples from a certain modality  $u$  that are “relevant” to the query sample  $x^{(v)}$  from modality  $v$ . We consider two samples to be relevant if they belong to the same class.

Denoting the modality of the query sample by  $v$  and the modality of the retrieved samples by  $u$ , we consider a retrieval strategy that returns the most relevant  $K$  samples to the query sample, based on the distance of the samples in the domain of embedding. Hence, given the query sample  $x^{(v)}$ , it is first embedded into  $\mathbb{R}^d$  as  $f^{(v)}(x^{(v)})$  via the interpolator  $f^{(v)}$ ; and then the  $K$  training samples  $\{x_i^{(u)}\}$  from modality  $u$  whose embeddings  $\{f^{(u)}(x_i^{(u)})\}$  have the smallest distance to  $f^{(v)}(x^{(v)})$  are retrieved as the most relevant samples, thus returning the set  $\{x_{i_k}^{(u)}\}_{k=1}^K$ , where

$$i_1 = \arg \min_i \|f^{(u)}(x_i^{(u)}) - f^{(v)}(x^{(v)})\|$$

$$i_k = \arg \min_{i \notin \{i_1, \dots, i_{k-1}\}} \|f^{(u)}(x_i^{(u)}) - f^{(v)}(x^{(v)})\|, \text{ for } k = 2, \dots, K. \quad (6)$$

The precision rate  $P$  and the recall rate  $R$  of the retrieval algorithm are then given by

$$P = \frac{TP}{TP + FP}, \quad R = \frac{TP}{TP + FN} \quad (7)$$

where  $TP$ ,  $FP$ , and  $FN$  respectively denote the number of true positive, false positive, and false negative samples

depending on whether the retrieved and unretrieved samples are relevant or not.

We present the following main result regarding the performance of cross-modal retrieval with supervised embeddings.

**Theorem 2.** *Let the training sample set  $\mathcal{X}$  contain  $N_m$  training samples  $\{x_i\}_{i=1}^{N_m}$  from class  $m$ , with observations  $\{x_i^{(v)}\}$  and  $\{x_i^{(u)}\}$  available in the modalities  $v$  and  $u$ . Let  $\mathcal{Y}$  be an embedding of  $\mathcal{X}$  in  $\mathbb{R}^d$  with the following properties:*

- (P1)  $\|y_i^{(v)} - y_i^{(u)}\| \leq \eta$  for all training samples  $x_i$
- (P2) For two samples  $x_i$  and  $x_j$  with  $C(x_i) = C(x_j)$ 

$$\|y_i^{(v)} - y_j^{(v)}\| \leq R_\delta \quad \text{if } \|x_i^{(v)} - x_j^{(v)}\| \leq 2\delta;$$

$$\|y_i^{(u)} - y_j^{(u)}\| \leq R_\delta \quad \text{if } \|x_i^{(u)} - x_j^{(u)}\| \leq 2\delta$$
- (P3)  $\|y_i^{(v)} - y_j^{(u)}\| > \gamma$  if  $C(x_i) \neq C(x_j)$ ,

where  $\eta$  and  $\gamma$  are some constants and  $R_\delta$  is a  $\delta$ -dependent constant. Assume that the interpolation functions  $f^{(v)} : H^{(v)} \rightarrow \mathbb{R}^d$  and  $f^{(u)} : H^{(u)} \rightarrow \mathbb{R}^d$  in modalities  $v$  and  $u$  are Lipschitz continuous with constant  $L$  such that for some parameters  $\epsilon > 0$  and  $\delta > 0$ , the following inequality holds

$$6L\delta + 2\sqrt{d}\epsilon + 2R_\delta + 2\eta \leq \gamma. \quad (8)$$

For some  $Q \geq 1$ , let the number of training samples from class  $m$  be such that

$$N_m > \frac{Q}{\eta_{m,\delta}}.$$

Let  $x^{(v)} \sim \nu_m^{(v)}$  be a query sample from class  $m$  observed in modality  $v$ , the relevant samples to which are sought in modality  $u$ . Then, with probability at least

$$1 - \exp\left(-\frac{2(N_m\eta_{m,\delta} - Q)^2}{N_m}\right) - 2d \exp\left(-\frac{Q\epsilon^2}{2L^2\delta^2}\right) - (1 - \eta_{m,\delta})^Q$$

the precision rate  $P$  of the retrieval algorithm in (6) satisfies

$$\begin{aligned} P &= 1, & \text{if } K \leq Q \\ P &\geq \frac{Q}{K}, & \text{if } K > Q \end{aligned} \quad (9)$$

and the recall rate  $R$  of the retrieval algorithm satisfies

$$\begin{aligned} R &= \frac{K}{N_m}, & \text{if } K \leq Q \\ R &\geq \frac{Q}{N_m}, & \text{if } K > Q. \end{aligned} \quad (10)$$

The proof of Theorem 2 is given in the Appendix. Theorem 2 can be interpreted similarly to Theorem 1. The properties (P1), (P2) and (P3) ensure that the learnt embedding aligns modalities  $v$  and  $u$  sufficiently well, while mapping nearby samples from the same classes to nearby points, and increasing the distance between samples from different classes. Assuming that the condition (8) is satisfied, the precision and recall rates given in (9) and (10) are attained with probability approaching 1 at an exponential rate as the number of training samples increases. In the proof of the theorem, the precision and recall rates in (9) and (10) are obtained by identifying the conditions

under which at least  $Q$  samples out of the  $K$  samples returned by the retrieval algorithm are relevant to the query sample.

The condition (8) required for successful cross-modal retrieval is the same as the condition (3) for accurate multi-modal classification. Hence, similarly to the findings of our multi-modal classification analysis, the results of our retrieval analysis also suggest that it is necessary to find a good compromise between the Lipschitz continuity of the interpolators and the separation between different classes when learning nonlinear embeddings for cross-modal retrieval applications.

#### IV. PROPOSED MULTI-MODAL SUPERVISED EMBEDDING METHOD

In this section, we propose a multi-modal nonlinear dimensionality reduction algorithm that relies on the theoretical findings of Section III. We formulate the nonlinear embedding problem in Section IV-A and then discuss its solution in Section IV-B.

##### A. Problem Formulation

Let  $X^{(v)} \in \mathbb{R}^{N^{(v)} \times n^{(v)}}$  denote the training data matrix of modality  $v$ , each row of which is the observation  $x_i^{(v)}$  of some training sample  $x_i$  in the  $v$ -th modality. Here  $N^{(v)}$  is the total number of observations<sup>2</sup> from all classes in modality  $v$ , and  $n^{(v)}$  is the dimension of the Hilbert space  $H^{(v)}$  of modality  $v$ , assumed to be finite in a practical setting. Given the training samples  $X^{(v)}$  from modalities  $v = 1, \dots, V$ , we would like to compute embeddings  $Y^{(v)} \in \mathbb{R}^{N^{(v)} \times d}$  of the training samples into the common domain  $\mathbb{R}^d$ , such that each  $x_i^{(v)} \in \mathbb{R}^{n^{(v)}}$  is mapped to a vector  $y_i^{(v)} \in \mathbb{R}^d$ . The embedding is extended to the whole data space through interpolation functions  $f^{(v)} : \mathbb{R}^{n^{(v)}} \rightarrow \mathbb{R}^d$  such that each training sample is mapped to its embedding as  $f^{(v)}(x_i^{(v)}) = y_i^{(v)}$ .

Our main purpose is to find an embedding that can be successfully generalized to initially unavailable test samples. We recall from our theoretical analysis that for successful generalization in multi-modal classification and retrieval, the embedding must have the properties (P1), (P2) and (P3) given in Theorems 1 and 2, while the Lipschitz constant of the interpolators must be kept sufficiently small as imposed by the conditions (3) and (8). We now formulate our multi-modal learning problem in the light of these results.

**Lipschitz regularity of the interpolators.** For the extension of the embedding, we choose to use RBF interpolation functions, which are analytical functions with well-studied properties. Hence, the interpolator of each modality  $v = 1, \dots, V$  has the form  $f^{(v)}(x^{(v)}) = [f_1^{(v)}(x^{(v)}) \dots f_d^{(v)}(x^{(v)})]$ , where

$$f_k^{(v)}(x^{(v)}) = \sum_{i=1}^{N^{(v)}} C_{ik}^{(v)} \phi^{(v)}(\|x^{(v)} - x_i^{(v)}\|) \quad (11)$$

is the  $k$ -th component of  $f^{(v)}(x^{(v)})$ . Here

$$\phi^{(v)}(r) = e^{-r^2/(\sigma^{(v)})^2}$$

<sup>2</sup>Although the observations of all training samples were assumed to be available in all modalities for the simplicity of the theoretical analysis in Section III, here we remove this assumption and allow some observations to be missing in some modalities. Hence  $N^{(v)}$  may be different for different  $v$ .

is a Gaussian RBF kernel with scale parameter  $\sigma^{(v)}$  and  $C_{ik}^{(v)}$  are the interpolator coefficients.

The Lipschitz continuity of Gaussian RBF interpolators has been studied in [38], from which it follows that  $f^{(v)}(x^{(v)})$  is Lipschitz-continuous with constant

$$L^{(v)} = \sqrt{2}e^{-\frac{1}{2}}\sqrt{N^{(v)}}(\sigma^{(v)})^{-1}\|C^{(v)}\|_F. \quad (12)$$

Here  $C^{(v)}$  is the coefficient matrix with entries  $C_{ik}^{(v)}$ . The interpolator coefficients can be easily obtained as

$$C^{(v)} = (\Psi^{(v)})^{-1}Y^{(v)}$$

by fitting the embedding coordinates  $Y^{(v)}$  to the training data  $X^{(v)}$ , where  $\Psi^{(v)} \in \mathbb{R}^{N^{(v)} \times N^{(v)}}$  is the RBF kernel matrix with entries  $\Psi_{ij}^{(v)} = \phi^{(v)}(\|x_i^{(v)} - x_j^{(v)}\|)$ .

The conditions (3) and (8) suggest that the Lipschitz constants of the interpolators should be sufficiently small for successful generalization of the embedding to test data. In view of these results, when learning a nonlinear embedding, we propose to minimize the kernel scale of each modality  $v$  through the term

$$\sum_{v=1}^V (\sigma^{(v)})^{-2}$$

as well as the interpolator coefficients of all modalities through

$$\sum_{v=1}^V \|C^{(v)}\|_F^2 = \sum_{v=1}^V \|(\Psi^{(v)})^{-1}Y^{(v)}\|_F^2 = \text{tr}(\tilde{Y}^T \tilde{\Psi}^{-2} \tilde{Y})$$

so that the Lipschitz constant  $L^{(v)}$  in (12) is minimized for each modality  $v$ . Here

$$\tilde{Y} = [(Y^{(1)})^T \ (Y^{(2)})^T \ \dots \ (Y^{(V)})^T]^T \in \mathbb{R}^{N \times d}$$

denotes the matrix containing the embeddings from all modalities (with  $N = \sum_v N^{(v)}$ ) and  $\tilde{\Psi} \in \mathbb{R}^{N \times N}$  is a block-diagonal matrix containing the kernel matrix  $\Psi^{(v)}$  in its  $v$ -th block.

**Within-class compactness.** Theorems 1 and 2 suggest that the constant  $R_\delta$  in (P2) should be kept small, so that the conditions (3) and (8) are more likely to be met. Although it is not easy to analytically formulate the minimization of  $R_\delta$ , in practice if nearby samples from the same modality and same class are embedded into nearby points,  $R_\delta$  will be small. This problem is well-studied in the manifold learning literature. The total weighted distance between the embeddings of same-class samples can be formulated as

$$\sum_{v=1}^V \sum_{i,j=1}^{N^{(v)}} (W_w^{(v)})_{ij} \|y_i^{(v)} - y_j^{(v)}\|^2 = \text{tr}(\tilde{Y}^T \tilde{L}_w \tilde{Y}). \quad (13)$$

Here  $W_w^{(v)} \in \mathbb{R}^{N^{(v)} \times N^{(v)}}$  is chosen as a weight matrix whose entries  $(W_w^{(v)})_{ij} = \exp(-\|x_i^{(v)} - x_j^{(v)}\|^2 / (\theta^{(v)})^2)$  represent the affinity between the data samples when  $x_i^{(v)}$  and  $x_j^{(v)}$  are from the same class (for a scale parameter  $\theta^{(v)}$ ), and  $(W_w^{(v)})_{ij} = 0$  otherwise. In the equality, the block-diagonal matrix  $\tilde{L}_w \in \mathbb{R}^{N \times N}$  contains the within-class Laplacian  $L_w^{(v)} = D_w^{(v)} - W_w^{(v)}$  in its  $v$ -th block, where  $D_w^{(v)}$  is the diagonal degree matrix with  $i$ -th diagonal entry given by  $\sum_j (W_w^{(v)})_{ij}$ . The term in (13) hence imposes nearby samples

$x_i^{(v)}, x_j^{(v)}$  from the same class and the same modality to be mapped to nearby coordinates.

**Between-class separation.** In Theorems 1 and 2, the between-class margin  $\gamma$  in (P3) must be sufficiently large for conditions (3) and (8) to be satisfied. Since it is difficult to formulate the maximization of the exact value of  $\gamma$ , we relax this problem to the maximization of

$$\sum_{v=1}^V \sum_{i,j=1}^{N^{(v)}} (W_b^{(v)})_{ij} \|y_i^{(v)} - y_j^{(v)}\|^2 = \text{tr}(\tilde{Y}^T \tilde{L}_b \tilde{Y})$$

which aims to increase the separation between the samples from different classes within each modality  $v$ . Here the matrix  $W_b^{(v)} \in \mathbb{R}^{N^{(v)} \times N^{(v)}}$  has entries  $(W_b^{(v)})_{ij} = 1$  when  $x_i^{(v)}$  and  $x_j^{(v)}$  are from different classes; and  $(W_b^{(v)})_{ij} = 0$ , otherwise. The block-diagonal matrix  $\tilde{L}_b \in \mathbb{R}^{N \times N}$  contains the between-class Laplacian  $L_b^{(v)} = D_b^{(v)} - W_b^{(v)}$  in its  $v$ -th block, where  $D_b^{(v)}$  is the diagonal between-class degree matrix with  $i$ -th diagonal entry given by  $\sum_j (W_b^{(v)})_{ij}$ .

**Cross-modal alignment.** Finally, the constant  $\eta$  in property (P1) in Theorems 1 and 2 should be sufficiently small for conditions (3) and (8) to be met. The parameter  $\eta$  represents the distance between the embeddings of the observations of the same sample in different modalities. We relax the minimization of  $\eta$  to the minimization of the following term, which aims to embed samples of high affinity from different modalities  $v, u$  into nearby points

$$\sum_{v=1}^V \sum_{u \neq v} \sum_{i=1}^{N^{(v)}} \sum_{j=1}^{N^{(u)}} (W_w^{(vu)})_{ij} \|y_i^{(v)} - y_j^{(u)}\|^2 = \text{tr}(\tilde{Y}^T \tilde{L}_{cw} \tilde{Y}).$$

Here, the matrix  $W_w^{(vu)} \in \mathbb{R}^{N^{(v)} \times N^{(u)}}$  encodes the affinities between sample pairs from different modalities.  $(W_w^{(vu)})_{ij}$  is nonzero only if  $x_i^{(v)}$  and  $x_j^{(u)}$  are from the same class, in which case it is computed with the Gaussian kernel based on the distance between  $x_i^{(v)}$  and  $x_j^{(u)}$  when transferred to a common modality (i.e., using  $\|x_i^{(v)} - x_j^{(u)}\|$  or  $\|x_i^{(u)} - x_j^{(u)}\|$ , otherwise  $\|x_i^{(r)} - x_j^{(r)}\|$  in some other modality  $r$  if the former ones are not possible). Denoting by  $\tilde{W}_{cw} \in \mathbb{R}^{N \times N}$  the cross-modal within-class weight matrix containing  $W_w^{(vu)}$  in its  $(v, u)$ -th block, the corresponding Laplacian matrix  $\tilde{L}_{cw} \in \mathbb{R}^{N \times N}$  is computed as  $\tilde{L}_{cw} = \tilde{D}_{cw} - \tilde{W}_{cw}$ , where  $\tilde{D}_{cw}$  is the diagonal degree matrix with  $i$ -th diagonal entry given by  $\sum_j (\tilde{W}_{cw})_{ij}$ .

Meanwhile, the property (P3) in Theorems 1 and 2 suggests that two samples from modalities  $v, u$  should be separated if they are from different classes. We thus propose to maximize

$$\sum_{v=1}^V \sum_{u \neq v} \sum_{i=1}^{N^{(v)}} \sum_{j=1}^{N^{(u)}} (W_b^{(vu)})_{ij} \|y_i^{(v)} - y_j^{(u)}\|^2 = \text{tr}(\tilde{Y}^T \tilde{L}_{cb} \tilde{Y})$$

where the matrix  $W_b^{(vu)} \in \mathbb{R}^{N^{(v)} \times N^{(u)}}$  is formed by setting  $(W_b^{(vu)})_{ij} = 1$  if  $x_i^{(v)}$  and  $x_j^{(u)}$  are from different classes, and 0 otherwise. The cross-modal between-class weight matrix  $\tilde{W}_{cb} \in \mathbb{R}^{N \times N}$  contains the matrix  $W_b^{(vu)}$  in its  $(v, u)$ -th block, while  $\tilde{L}_{cb} \in \mathbb{R}^{N \times N}$  is the corresponding Laplacian matrix given by  $\tilde{L}_{cb} = \tilde{D}_{cb} - \tilde{W}_{cb}$ , with  $\tilde{D}_{cb}$  denoting the diagonal degree matrix with  $i$ -th diagonal entry given by  $\sum_j (\tilde{W}_{cb})_{ij}$ .

**Overall problem.** We now combine all these objectives in the following overall optimization problem

$$\begin{aligned} & \underset{\tilde{Y}, \{\sigma^{(v)}\}}{\text{minimize}} \quad \text{tr}(\tilde{Y}^T \tilde{L}_w \tilde{Y}) - \mu_1 \text{tr}(\tilde{Y}^T \tilde{L}_b \tilde{Y}) + \mu_2 \text{tr}(\tilde{Y}^T \tilde{\Psi}^{-2} \tilde{Y}) \\ & + \mu_3 \sum_{v=1}^V (\sigma^{(v)})^{-2} + \mu_4 \text{tr}(\tilde{Y}^T \tilde{L}_{cw} \tilde{Y}) - \mu_5 \text{tr}(\tilde{Y}^T \tilde{L}_{cb} \tilde{Y}) \quad (14) \end{aligned}$$

subject to  $\tilde{Y}^T \tilde{Y} = I$ , where  $\mu_1, \dots, \mu_5$  are positive weight parameters,  $I \in \mathbb{R}^{d \times d}$  is the identity matrix, and the optimization constraint  $\tilde{Y}^T \tilde{Y} = I$  is for the normalization of the learnt coordinates.

### B. Solution of the Optimization Problem

Defining

$$A = \tilde{L}_w - \mu_1 \tilde{L}_b + \mu_2 \tilde{\Psi}^{-2} + \mu_4 \tilde{L}_{cw} - \mu_5 \tilde{L}_{cb} \quad (15)$$

the problem in (14) can be rewritten as

$$\underset{\tilde{Y}, \{\sigma^{(v)}\}}{\text{minimize}} \quad \text{tr}(\tilde{Y}^T A \tilde{Y}) + \mu_3 \sum_{v=1}^V (\sigma^{(v)})^{-2}, \quad \text{subject to } \tilde{Y}^T \tilde{Y} = I. \quad (16)$$

The above problem is not jointly convex in  $\tilde{Y}$  and  $\{\sigma^{(v)}\}$ , hence it is not easy to find its global optimum. We minimize the objective function with an iterative alternating optimization scheme, where we first optimize  $\tilde{Y}$  by fixing  $\{\sigma^{(v)}\}$ , and then optimize  $\{\sigma^{(v)}\}$  by fixing  $\tilde{Y}$  in each iteration as follows.

**Optimization of  $\tilde{Y}$ :** When  $\{\sigma^{(v)}\}$  are fixed, the optimization problem in (16) becomes

$$\underset{\tilde{Y}}{\text{minimize}} \quad \text{tr}(\tilde{Y}^T A \tilde{Y}) \quad \text{subject to } \tilde{Y}^T \tilde{Y} = I. \quad (17)$$

The solution to this problem is given by the  $d$  eigenvectors of the matrix  $A$  corresponding to its smallest  $d$  eigenvalues.

**Optimization of  $\{\sigma^{(v)}\}$ :** Fixing  $\tilde{Y}$ , the problem (16) becomes

$$\underset{\{\sigma^{(v)}\}}{\text{minimize}} \quad \mu_2 \text{tr}(\tilde{Y}^T \tilde{\Psi}^{-2} \tilde{Y}) + \mu_3 \sum_{v=1}^V (\sigma^{(v)})^{-2}. \quad (18)$$

Note that the first term in the objective depends on the kernel scale parameters  $\{\sigma^{(v)}\}$  through the entries of the kernel matrix  $\tilde{\Psi}$ . Due to the block diagonal structure of  $\tilde{\Psi}$  and the separability of the second term, the objective (18) can be decomposed into  $V$  individual objectives, each one of which is a function of only one scale parameter  $\sigma^{(v)}$ . We minimize these objective functions one by one, by optimizing one scale parameter  $\sigma^{(v)}$  at a time through exhaustive search.

If  $\mu_1$  and  $\mu_5$  are sufficiently small, the matrix  $A$  becomes positive semi-definite. In this case, the objective function is guaranteed to converge since it is nonnegative, and both updates on  $\tilde{Y}$  and  $\{\sigma^{(v)}\}$  reduce it. We continue the iterations until the convergence of the objective. We call the proposed algorithm Multi-modal Nonlinear Supervised Embedding (MNSE), which is summarized in Algorithm 1.

### Algorithm 1 Multi-modal Nonlinear Supervised Embedding (MNSE)

---

**Input:** Training data matrices  $\{X^{(v)}\}$  and training data labels  
**Initialization:**  
 Obtain the graph Laplacian matrices  $\tilde{L}_w, \tilde{L}_b, \tilde{L}_{cw}$ , and  $\tilde{L}_{cb}$ .  
 Assign weight parameters  $\{\mu_1, \mu_2, \dots, \mu_5\}$ , and initial kernel scales  $\sigma^{(v)}$   
**repeat**  
   Compute the nonlinear embeddings  $\tilde{Y}$  through (17) by fixing  $\{\sigma^{(v)}\}$   
   Compute the kernel scale parameters  $\{\sigma^{(v)}\}$  through (18) by fixing  $\tilde{Y}$   
**until** the maximum number of iterations or the convergence of the objective  
**Output:**  
 Kernel scale parameters  $\sigma^{(v)}$  and projected training data  $Y^{(v)}$   
 Kernel coefficients  $C^{(v)} = (\Psi^{(v)})^{-1} Y^{(v)}$

---

### C. Complexity Analysis

The complexity of the proposed MNSE method is mainly determined by those of the problems (17) and (18) repeated in the main loop of the algorithm. When computing the matrix  $A$  in (15), the matrices  $\tilde{L}_w, \tilde{L}_b, \tilde{\Psi}, \tilde{L}_{cw}$ , and  $\tilde{L}_{cb}$  can be constructed with complexity not exceeding  $O(N^2)$ , where  $N = \sum_v N^{(v)}$  is the total number of observations from all modalities. The eigenvalue decomposition step in (17) is of complexity  $O(N^3)$ . In the optimization problem (18), the evaluation of the objective for each  $\sigma^{(v)}$  value requires  $O((N^{(v)})^3)$  operations in modality  $v$ ; hence, the total complexity of finding all  $\{\sigma^{(v)}\}$  is smaller than  $O(N^3)$ . Therefore, the overall complexity of the algorithm is determined as  $O(N^3)$ .

## V. EXPERIMENTAL RESULTS

We first study the stabilization of the proposed MNSE algorithm and its sensitivity to the algorithm parameters in Section V-A. Then, we evaluate its performance with comparative experiments in multi-view image classification and image-text retrieval applications in Section V-B.

### A. Stabilization and Sensitivity Analysis of MNSE

We analyze the performance of MNSE in an image classification setting. The experiments are done on the MIT-CBCL multi-view face data set [40], which contains face images of 10 participants captured under 36 illumination conditions and 9 different pose angles. Images with frontal and profile poses are used in the experiments, which are considered to represent two different modalities. Some sample images of two participants in both modalities are shown in Figure 2. The images in each modality are randomly divided into 100 training and 260 test images in each experiment. The embedding parameters are computed using the training images, which are then applied to the test images to estimate their class labels via NN classification. The misclassification errors obtained with the representations of the images in Modalities 1 and 2 are reported individually. The reported results are the average of 10 random trials.

We first study in Figure 3 the evolution of the objective function of (14) and the misclassification error (in percentage)

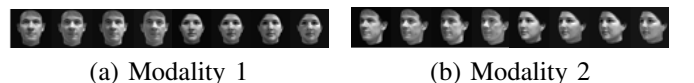


Fig. 2. Sample images from the MIT-CBCL face data set



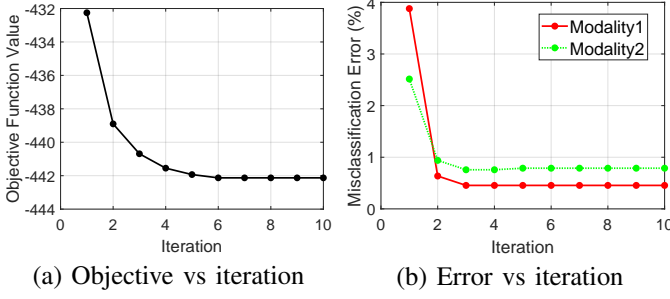


Fig. 3. The evolutions of the objective function and the misclassification error during the iterations for the MIT-CBCL data set

of the test images throughout the optimization iterations. Figure 3(a) indicates that the overall objective function steadily decreases throughout the iterations as expected, confirming the efficacy of the proposed optimization procedure. The updates on both the embeddings  $\{Y^{(v)}\}$  and the kernel scale parameters  $\{\sigma^{(v)}\}$  ensure that the overall objective decreases or remains constant. The misclassification errors in Figure 3(b) are seen to decrease rather regularly during the iterations, in line with the decrease in the objective. This suggests that the proposed objective function is indeed well-representative of the classification error of the algorithm.

Next, the effect of the weight parameters  $\mu_1, \mu_2, \dots, \mu_5$  on the algorithm performance is studied in Figure 4. Figure 4(a) shows the variation of the misclassification error with  $\mu_2$  and  $\mu_3$ , by fixing  $\mu_1 = 10^2$ ,  $\mu_4 = 1$ , and  $\mu_5 = 10^2$ . Similarly, 4(b) shows the variation of the error with  $\mu_4$  and  $\mu_1 = \mu_5$ , by fixing  $\mu_2 = 10^{-2}$  and  $\mu_3 = 1$ . The parameters  $\mu_1$  and  $\mu_5$  are set to be equal, motivated by the similarity in the construction of the between-class separation matrices associated with these parameters. Figure 4(a) indicates that the weight  $\mu_2$  of the squared norms  $\|C^{(v)}\|_F^2$  of the interpolator coefficient matrices should be relatively low ( $\mu_2 \in [10^{-3}, 1]$ ), while the weight  $\mu_3$  for the kernel scale parameter terms  $(\sigma^{(v)})^{-2}$  should be higher ( $\mu_3 \in [10^{-1}, 10^1]$ ). This can be explained in the way that an appropriate assignment of  $\mu_2$  and  $\mu_3$  should balance the orders of the magnitudes of their corresponding terms in the objective, which are significantly different. Figure 4(b) suggests that the weight parameter  $\mu_4$  of the cross-modal within-class similarity term and the weight parameters  $\mu_1, \mu_5$  for the between-class discrimination terms can be chosen in a rather large region ( $\mu_1 = \mu_5 \in [10^{-1}, 10^3]$  and  $\mu_4 \in [1, 10^3]$ ) without much loss in the performance. This shows that the algorithm performance is relatively robust with respect to the choice of these parameters.

Finally, we examine the effect of the dimension  $d$  of the embedding on the misclassification error in Figure 5. The results show that the algorithm performs well for  $d \geq 9$ . Since choosing a small  $d$  value has the advantage of reducing the computational load and avoiding potential overfitting issues, the embedding dimension is chosen as  $d = 9$  in all experiments in the next section.

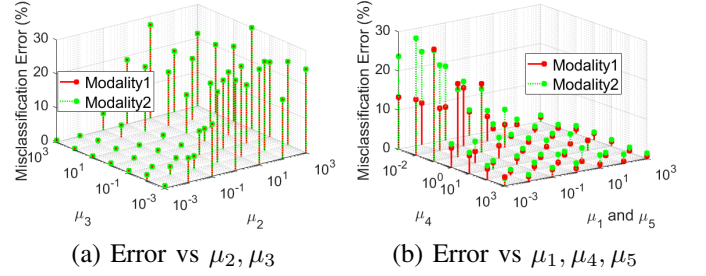


Fig. 4. The variation of the misclassification error with the weight parameters  $\mu_1, \mu_2, \mu_3, \mu_4, \mu_5$  for the MIT-CBCL data set

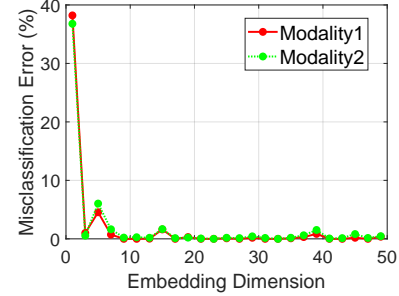


Fig. 5. The variation of the misclassification error with the embedding dimension  $d$  for the MIT-CBCL face data set

### B. Evaluation of the Algorithm Performance

We now evaluate the performance of the proposed MNSE algorithm with comparative experiments in image classification and image-text retrieval applications. MNSE is compared to the multi-modal representation learning algorithms CCA, Kernel CCA [1], GMLDA [2], JFSSL [3], DeepMF [37], as well as the baseline single-modal methods PCA, NN classification in the original domain, and NSSE [38]. The multi-modal CCA and GMLDA algorithms are applied after a preprocessing step of dimensionality reduction with PCA, which has been seen to improve the performance of these two algorithms. For the multi-modal methods, nonlinear embeddings of different modalities into a common domain are learnt with the training data, which are then used for embedding the test data. The single-modal methods are applied independently in each modality. The parameters of the compared algorithms are optimized for the best performance. The weight parameters of the proposed MNSE algorithm are selected within the regions suggested in Section V-A.

1) *Multi-modal image classification:* The multi-modal classification experiments are done on the MIT-CBCL face data set described in Section V-A. The data set is separated randomly into training and test sets at different ratios. The weight parameters of the proposed MNSE method are chosen as  $\mu_1 = 10^2$ ,  $\mu_2 = 10^{-3}$ ,  $\mu_3 = 1$ ,  $\mu_4 = 10^2$ ,  $\mu_5 = 10^2$ . In the test stage, a scenario is considered where a test image is available in only one modality. Test images are embedded into the common domain with the learnt projections and are classified with NN classification using the embeddings of the training samples of their own modality. Table I shows the misclassification errors (in percentage) of test images for

TABLE I  
MISCLASSIFICATION ERRORS (%) OF COMPARED METHODS FOR THE MIT-CBCL DATA SET. TOP AND BOTTOM ROWS SHOW THE ERRORS OBTAINED WITH MODALITIES 1 AND 2.

Algorithm	Training size				
	5.6%	8.3%	11.1%	13.9%	27.8%
NN	22.12 19.68	19 17.64	10.69 6.94	2.97 1.71	0.77 0
PCA	3.68 4.29	0.06 0.54	0.34 0.06	0.10 0	0 0
NSSE [38]	1.94 4.56	0.03 1	0.03 0.09	0 0.03	0 0
CCA [1]	3.67 4.29	0.06 0.55	0.34 0.06	0.10 0	0 0
Kernel CCA [1]	1.5 4	0.21 0.72	0.21 0.66	0.09 0.39	0 0.19
GMLDA [2]	0 0.30	0 0.06	0 0.03	0 0	0 0
JFSSL [3]	0 0.12	0 0	0 0	0 0	0 0
DeepMF [37]	5.15 8.50	1.52 3.42	0.63 1.03	0.39 0.84	0 0
MNSE	0.15 1.35	0 0.27	0 0.03	0 0	0 0

different training sizes (ratio of the training samples in the data set), obtained with their representations in Modalities 1 and 2. The results are averaged over 10 random repetitions of the experiment.

The results in Table I show that the proposed MNSE method outperforms all single-modal methods, as well as the multi-modal CCA, Kernel CCA, and DeepMF methods in both setups. The comparison between MNSE and the single-modal NSSE method is particularly interesting. Both methods compute nonlinear smooth interpolation functions and perform the final NN classification with the embeddings of training samples from only one modality. However, MNSE fuses the information from both modalities in the training phase, unlike the single-modal NSSE. The fact that MNSE outperforms NSSE confirms that it can successfully exploit and combine the information from both modalities when optimizing the embedding parameters. Being linear and supervised multi-modal methods, JFSSL and GMLDA yield similar classification performance to MNSE, where the error of all three methods are quite small (within 0%–1.35%). However, JFSSL and GMLDA are observed to outperform MNSE at very small training sizes. As MNSE is a nonlinear method incorporating a relatively rich model with more parameters to learn, it requires more training samples than these two simpler methods learning only linear projections. Also, the approach underlying JFSSL and GMLDA, i.e., aligning the modalities via linear projections, is particularly suited to this synthetic and regularly structured face data set, as the images viewing the same participants from different angles are quite convenient to align via linear transformations. Among the nonlinear multi-modal methods, the proposed MNSE performs better than the unsupervised Kernel CCA and DeepMF methods, which do not exploit the information of the class labels.

2) *Cross-modal image-text retrieval*: The retrieval experiments are done on the Wikipedia [41] and Pascal VOC2007 [42] image-text data sets. The Wikipedia data set contains 2866 image-text pairs describing the contents of the articles, which are categorized into 10 classes. 128-dimensional SIFT

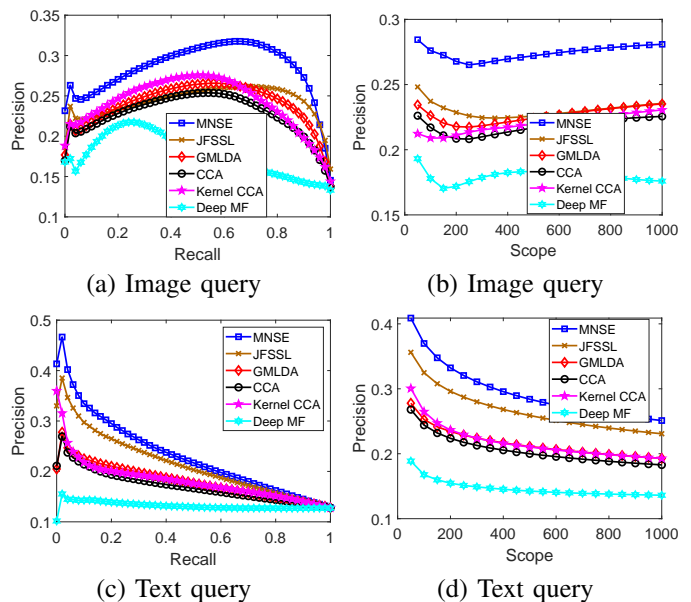


Fig. 6. Retrieval performance of the methods for the Wikipedia data set

TABLE II  
MAP SCORES FOR THE WIKIPEDIA DATA SET

Algorithm	CCA [1]	Kernel CCA [1]	GMLDA [2]	JFSSL [3]	DeepMF [37]	MNSE
Image Query	0.2280	0.2419	0.2407	0.2440	0.1760	<b>0.2847</b>
Text Query	0.1720	0.1815	0.1815	0.2143	0.1335	<b>0.2321</b>

histogram features are used in the image modality, and 10-dimensional text features obtained with a latent Dirichlet allocation model are used in the text modality [43], [44]. We randomly separate the image-text pairs into 1300 training and 1566 test pairs and average the results over 10 trials. The Pascal VOC2007 data set contains image-text pairs from 20 different object classes, where the experiments are done on 2808 training and 2841 test pairs whose images contain only one object. GIST feature vectors in the image modality and word count feature vectors in the text modality are used in the experiments. The weight parameters of MNSE are chosen as  $\mu_1 = 10^{-1}$ ,  $\mu_2 = 1$ ,  $\mu_3 = 1$ ,  $\mu_4 = 1$ ,  $\mu_5 = 10^{-1}$  for both data sets. In the training phase of the DeepMF algorithm on the Pascal VOC2007 data set, multiple pairs with the same word count features are reduced to a single pair via random selection in order to comply with the expected input format of this method, and the performance of the algorithm is evaluated on this reduced data set. The parameters of DeepMF are selected as proposed in [37], except for the layer size parameters which are adjusted to improve the performance on both data sets.

Embedding functions are learnt using the training set with the multi-modal methods under comparison. Then, the retrieval task is performed on the test set, by searching the relevant matches of an image query in the text database (based on the nearest neighbors in the common domain of embedding) for image-text retrieval, and vice versa for text-image retrieval. The precision and recall rates are computed as in (7) by considering a retrieved item relevant if it is from the same class as the query. Figures 6 and 7 show the precision-recall and

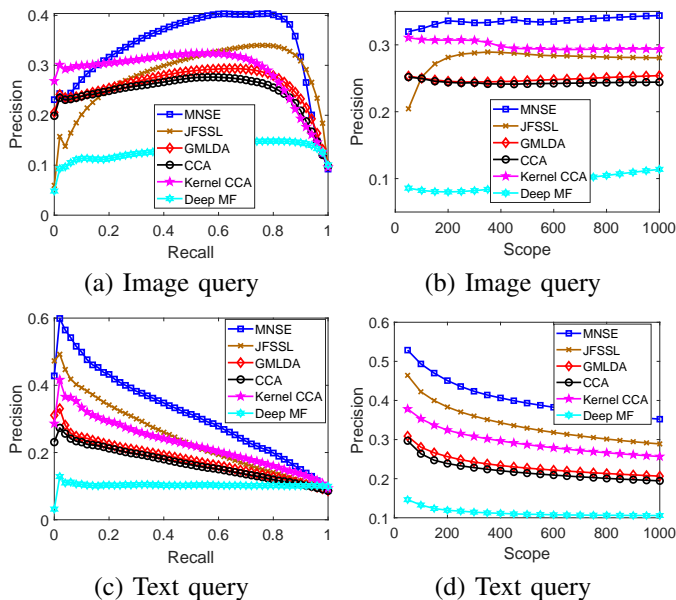


Fig. 7. Retrieval performance of the methods for the Pascal VOC2007 data set

TABLE III  
MAP SCORES FOR THE PASCAL VOC2007 DATA SET

Algorithm	CCA [1]	Kernel CCA [1]	GMLDA [2]	JFSSL [3]	DeepMF [37]	MNSE
Image Query	0.2470	0.2873	0.2609	0.2814	0.1305	<b>0.3390</b>
Text Query	0.1674	0.2282	0.1791	0.2418	0.1038	<b>0.3159</b>

precision-scope curves for both types of queries, respectively on the Wikipedia and the Pascal VOC2007 data sets. Tables II and III report the MAP (Mean Average Precision) scores of the methods, computed by averaging all average precision values over all query samples.

The results show that the proposed MNSE method outperforms all other multi-modal methods on both data sets. In contrast to the MIT-CBCL face data set used in image classification experiments, the Wikipedia and Pascal VOC2007 data sets have more diverse and irregular structures, with the two modalities bearing much less resemblance. This makes the multi-modal representation learning task more challenging, where the flexibility of the proposed nonlinear supervised embedding approach brings clear advantages over the other multi-modal methods in comparison. Among the supervised methods, the performance gap between the proposed nonlinear MNSE method and the linear JFSSL and GMLDA algorithms can be explained in the way that nonlinear representations capture the intricate geometries of these two challenging data sets significantly better than linear representations, while JFSSL and GMLDA performed quite well on the MIT-CBCL data set of much simpler structure. Among the nonlinear methods, the performances of the unsupervised Kernel CCA and DeepMF methods are behind that of the supervised MNSE. The fact that the relatively simpler Kernel CCA outperforms the more sophisticated DeepMF can be interpreted in the way that elaborate methods involving rich models may be preferable to simple methods only on large data collections, while simple

representation models can be learnt more successfully on relatively small data sets. The proposed MNSE method seems to offer a good compromise in this regard, between the richness of the representation models to be learnt and the ease of learning them.

## VI. CONCLUSION

We have first proposed a theoretical analysis of the performance of multi-modal supervised embedding methods in multi-modal classification and cross-modal retrieval applications. The main finding of our performance bounds is that achieving good between-class separation and cross-modal alignment is not sufficient, and the regularity of the multi-modal interpolation functions is also important for ensuring good generalization performance. Next, relying on these theoretical findings, we have proposed an algorithm for learning supervised multi-modal nonlinear embeddings, with particular focus on the generalizability of the learnt representations to new test samples. The efficacy of the proposed method has been demonstrated in multi-modal classification and cross-modal retrieval problems, where it has been shown to yield quite satisfactory performance in comparison with recent multi-modal learning algorithms. We hope that our theoretical insights along with our methodological contributions will be useful towards improving the interpretability and the performance of nonlinear representation learning algorithms in multiple domains.

## REFERENCES

- [1] C. Xu, D. Tao, and C. Xu, "A survey on multi-view learning," *arXiv Preprint*, 2013.
- [2] A. Sharma, A. Kumar, H. Daumé, and D. W. Jacobs, "Generalized multiview analysis: A discriminative latent space," in *Proc. IEEE Conference on Computer Vision and Pattern Recognition*, 2012, pp. 2160–2167.
- [3] K. Wang, R. He, L. Wang, W. Wang, and T. Tan, "Joint feature selection and subspace learning for cross-modal retrieval," *IEEE Trans. Pattern Anal. Mach. Intell.*, vol. 38, no. 10, pp. 2010–2023, 2016.
- [4] J. Ngiam, A. Khosla, M. Kim, J. Nam, H. Lee, and A. Y. Ng, "Multimodal deep learning," in *Proceedings of the 28th International Conference on Machine Learning*, 2011, pp. 689–696.
- [5] Y. Wei, Y. Zhao, C. Lu, S. Wei, L. Liu, Z. Zhu, and S. Yan, "Cross-modal retrieval with CNN visual features: A new baseline," *IEEE Trans. Cybernetics*, vol. 47, no. 2, pp. 449–460, 2017.
- [6] F. Feng, X. Wang, and R. Li, "Cross-modal retrieval with correspondence autoencoder," in *Proc. ACM International Conference on Multimedia*, 2014, pp. 7–16.
- [7] E. Vural and C. Guillemot, "A study of the classification of low-dimensional data with supervised manifold learning," *Journal of Machine Learning Research*, vol. 18, no. 373, pp. 1–55, 2018.
- [8] A. Blum and T. Mitchell, "Combining labeled and unlabeled data with co-training," in *Proc. 11th Annual Conference on Computational Learning Theory, COLT*, 1998, pp. 92–100.
- [9] K. Nigam and R. Ghani, "Analyzing the effectiveness and applicability of co-training," in *Proc. 9th Int. Conf. Information and Knowledge Management*, 2000, pp. 86–93.
- [10] U. Brefeld and T. Scheffer, "Co-EM support vector learning," in *Proc. 21st Int. Conf. Mach. Learn.*, 2004.
- [11] Z. Zhou and M. Li, "Semi-supervised regression with co-training," in *Proc. 19th International Joint Conference on Artificial Intelligence*, 2005, pp. 908–913.
- [12] S. Yu, B. Krishnapuram, R. Rosales, and R. B. Rao, "Bayesian co-training," *Journal of Machine Learning Research*, vol. 12, pp. 2649–2680, 2011.

- [13] N. Poh, J. Kittler, and A. Rattani, "Handling session mismatch by fusion-based co-training: An empirical study using face and speech multimodal biometrics," in *IEEE Symposium on Computational Intelligence in Biometrics and Identity Management*, 2014, pp. 81–86.
- [14] R. Yan and M. R. Naphade, "Multi-modal video concept extraction using co-training," in *Proc. IEEE International Conference on Multimedia and Expo*, 2005, pp. 514–517.
- [15] X. Duan, N. B. Thomsen, Z. Tan, B. Lindberg, and S. H. Jensen, "Weighted score based fast converging co-training with application to audio-visual person identification," in *IEEE 29th Int. Conf. Tools with Artif. Intel.*, 2017, pp. 610–617.
- [16] N. Rasiwasia, D. Mahajan, V. Mahadevan, and G. Aggarwal, "Cluster canonical correlation analysis," in *Proc. 17th Int. Conf. Artificial Intelligence and Statistics*, 2014, pp. 823–831.
- [17] V. Ranjan, N. Rasiwasia, and C. V. Jawahar, "Multi-label cross-modal retrieval," in *IEEE Int. Conf. Computer Vision*, 2015, pp. 4094–4102.
- [18] Y. Gong, Q. Ke, M. Isard, and S. Lazebnik, "A multi-view embedding space for modeling internet images, tags, and their semantics," *International Journal of Computer Vision*, vol. 106, no. 2, pp. 210–233, 2014.
- [19] J. Hu, J. Lu, and Y. Tan, "Sharable and individual multi-view metric learning," *IEEE Trans. Pattern Anal. Mach. Intell.*, vol. 40, no. 9, pp. 2281–2288, 2018.
- [20] D. Hidru and A. Goldenberg, "EquiNMF: Graph regularized multiview nonnegative matrix factorization," *arXiv Preprint*, 2014.
- [21] M. Kuss and T. Graepel, "The geometry of kernel canonical correlation analysis," *Technical report No. 108, Max Planck Institute for Biological Cybernetics*, 05 2003.
- [22] A. Argyriou, M. Herbster, and M. Pontil, "Combining graph laplacians for semi-supervised learning," in *Adv. Neural Inf. Proc. Sys. 18*, 2005, pp. 67–74.
- [23] P. Mercado, F. Tudisco, and M. Hein, "Generalized matrix means for semi-supervised learning with multilayer graphs," in *Adv. Neur. Inf. Proc. Sys. 32*, 2019, pp. 14848–14857.
- [24] K. P. Bennett, M. Momma, and M. J. Embrechts, "Mark: A boosting algorithm for heterogeneous kernel models," in *Proc. KDD-2002: Knowledge Discovery and Data Mining*, 2002, pp. 24–31.
- [25] G. Lanckriet, N. Cristianini, P. Bartlett, L. El Ghaoui, and M. Jordan, "Learning the kernel matrix with semidefinite programming," *Journal of Machine Learning Research*, vol. 5, pp. 27–72, 2004.
- [26] F. R. Bach and G. Lanckriet, "Multiple kernel learning, conic duality, and the SMO algorithm," in *Proc. 21st International Conference on Machine Learning*, 2004.
- [27] S. Sonnenburg, G. Rätsch, C. Schäfer, and B. Schölkopf, "Large scale multiple kernel learning," *Journal of Machine Learning Research*, vol. 7, pp. 1531–1565, 2006.
- [28] Z. Xu, R. Jin, H. Yang, I. King, and M. Lyu, "Simple and efficient multiple kernel learning by group Lasso," in *Proc. 27th International Conference on Machine Learning*, 2010, pp. 1175–1182.
- [29] T. Xia, D. Tao, T. Mei, and Y. Zhang, "Multiview spectral embedding," *IEEE Trans. Systems, Man, and Cybernetics, Part B*, vol. 40, no. 6, pp. 1438–1446, 2010.
- [30] L. Liu, F. Nie, A. Wiliem, Z. Li, T. Zhang, and B. C. Lovell, "Multi-modal joint clustering with application for unsupervised attribute discovery," *IEEE Transactions on Image Processing*, vol. 27, no. 9, pp. 4345–4356, 2018.
- [31] W. Wang, X. Yang, B. C. Ooi, D. Zhang, and Y. Zhuang, "Effective deep learning-based multi-modal retrieval," *The VLDB Journal*, vol. 25, no. 1, pp. 79–101, 2016.
- [32] S. Rastegar, M. S. Baghshah, H. R. Rabiee, and S. M. Shojaei, "MDL-CW: A multimodal deep learning framework with crossweights," in *Proc. IEEE Conf. Comp. Vis. Pattern Rec.*, 2016, pp. 2601–2609.
- [33] L. Castrejón, Y. Aytar, C. Vondrick, H. Pirsiavash, and A. Torralba, "Learning aligned cross-modal representations from weakly aligned data," in *Proc. IEEE Conference on Computer Vision and Pattern Recognition*, 2016, pp. 2940–2949.
- [34] Y. Niu, Z. Lu, J. Wen, T. Xiang, and S. Chang, "Multi-modal multi-scale deep learning for large-scale image annotation," *IEEE Trans. Image Processing*, vol. 28, no. 4, pp. 1720–1731, 2019.
- [35] C. Zhang, J. Cheng, and Q. Tian, "Multi-view image classification with visual, semantic and view consistency," *IEEE Trans. Image Processing*, vol. 29, pp. 617–627, 2020.
- [36] F. Yang, J. Chang, C. Tsai, and Y. F. Wang, "A multi-domain and multi-modal representation disentangler for cross-domain image manipulation and classification," *IEEE Trans. Image Processing*, vol. 29, pp. 2795–2807, 2020.
- [37] H. Zhao, Z. Ding, and Y. Fu, "Multi-view clustering via deep matrix factorization," in *Proc. Thirty-First AAAI Conf. Artif. Intel.*, 2017, pp. 2921–2927, AAAI Press.
- [38] C. Örnek and E. Vural, "Nonlinear supervised dimensionality reduction via smooth regular embeddings," *Pattern Recognition*, vol. 87, pp. 55–66, 2019.
- [39] S. Kaya and E. Vural, "Multi-modal learning with generalizable nonlinear dimensionality reduction," in *IEEE Int. Conf. Image Proc.*, 2019, pp. 2139–2143.
- [40] "MIT-CBCL face recognition database," Available: <http://cbcl.mit.edu/software-datasets/heisele/facerecognition-database.html>.
- [41] N. Rasiwasia, J. C. Pereira, E. Coviello, G. Doyle, G. Lanckriet, R. Levy, and N. Vasconcelos, "A New Approach to Cross-Modal Multimedia Retrieval," in *ACM International Conference on Multimedia*, 2010, pp. 251–260.
- [42] M. Everingham, L. Van Gool, C. K. I. Williams, J. Winn, and A. Zisserman, "The PASCAL Visual Object Classes Challenge 2007 (VOC2007) Results," <http://www.pascal-network.org/challenges/VOC/voc2007/workshop/index.html>.
- [43] D. M. Blei, A. Y. Ng, and M. I. Jordan, "Latent Dirichlet allocation," *Journal of Machine Learning Research*, vol. 3, pp. 993–1022, 2003.
- [44] K. Wang, Q. Yin, W. Wang, S. Wu, and L. Wang, "A comprehensive survey on cross-modal retrieval," *arXiv Preprint*, 2016.
- [45] R. Herbrich, "Exact tail bounds for binomial distributed variables," *Online: Available at <http://research.microsoft.com/apps/pubs/default.aspx?id=66854>*, 1999.

## APPENDIX

### Proof of Lemma 1

*Proof.* For an arbitrary modality  $u \in \{1, \dots, V\}$ , the observation  $x_i^{(u)}$  of a training sample  $x_i$  from class  $m$  drawn independently from the test sample  $x$  lies in a  $\delta$ -neighborhood of  $x^{(u)}$  with probability

$$P\left(x_i^{(u)} \in B_\delta(x^{(u)})\right) = \nu_m^{(u)}\left(B_\delta(x^{(u)})\right) \geq \eta_{m,\delta}.$$

Then, the probability that  $B_\delta(x^{(u)})$  contains at least  $Q$  samples among the  $N_m$  training samples drawn from  $\nu_m^{(u)}$  is given by

$$\begin{aligned} P(|A^{(u)}| \geq Q) &= \sum_{k=Q}^{N_m} \binom{N_m}{k} \left(\nu_m^{(u)}(B_\delta(x^{(u)}))\right)^k \left(1 - \nu_m^{(u)}(B_\delta(x^{(u)}))\right)^{N_m-k} \\ &\geq \sum_{k=Q}^{N_m} \binom{N_m}{k} (\eta_{m,\delta})^k (1 - \eta_{m,\delta})^{N_m-k}. \end{aligned}$$

This is obtained by evaluating the probability that at least  $Q$  successes occur within  $N_m$  independent Bernoulli trials with success probability more than  $\eta_{m,\delta}$  in each trial. Following the approach in the proof of [7, Theorem 5], from the assumption  $N_m > \frac{Q}{\eta_{m,\delta}}$ , we can lower bound this probability using a tail bound for distributions [45]. We thus get

$$P(|A^{(u)}| \geq Q) \geq 1 - \exp\left(-\frac{2(N_m\eta_{m,\delta} - Q)^2}{N_m}\right).$$

Now assume that the event  $|A^{(u)}| \geq Q$  has occurred for the modality  $u$ , i.e., there are at least  $Q$  training samples from class  $m$  within a  $\delta$ -neighborhood of  $x^{(u)}$ . Then, from [7, Lemma 3], with probability at least

$$1 - 2d \exp\left(-\frac{|A^{(u)}|\epsilon^2}{2L^2\delta^2}\right) \geq 1 - 2d \exp\left(-\frac{Q\epsilon^2}{2L^2\delta^2}\right)$$

the distance between  $f^{(u)}(x^{(u)})$  and the sample average of the embeddings of its neighboring training samples is bounded as

$$\left\| f^{(u)}(x^{(u)}) - \frac{1}{|A^{(u)}|} \sum_{x_i^{(u)} \in A^{(u)}} f^{(u)}(x_i^{(u)}) \right\| \leq L\delta + \sqrt{d}\epsilon. \quad (19)$$

Next, still assuming that the event  $|A^{(u)}| \geq Q$  has occurred for the modality  $u$ , for each sample  $x_i^{(u)} \in A^{(u)}$ , the probability that its observation  $x_i^{(v)}$  in modality  $v$  is outside  $B_\delta(x^{(v)})$  is

$$1 - \nu_m^{(v)}(B_\delta(x^{(v)})) \leq 1 - \eta_{m,\delta}.$$

Therefore, with probability at least  $1 - (1 - \eta_{m,\delta})^Q$ , there is at least one  $x_l^{(u)} \in B_\delta(x^{(u)})$  whose observation in modality  $v$  satisfies  $x_l^{(v)} \in B_\delta(x^{(v)})$ , or equivalently,  $\|x_l^{(v)} - x^{(v)}\| \leq \delta$ . Combining the probability expressions we obtained so far, we conclude that for an arbitrary modality  $q$ , with probability at least

$$1 - \exp\left(-\frac{2(N_m\eta_{m,\delta} - Q)^2}{N_m}\right) - 2d \exp\left(-\frac{Q\epsilon^2}{2L^2\delta^2}\right) - (1 - \eta_{m,\delta})^Q$$

we have  $|A^{(u)}| \geq Q$ , the event in (19) occurs, and there is at least one  $x_l^{(u)} \in B_\delta(x^{(u)})$  such that  $\|x_l^{(v)} - x^{(v)}\| \leq \delta$ .  $\square$

### Proof of Theorem 1

*Proof.* We first recall from Lemma 1 that for a particular modality  $u \in \{1, \dots, V\}$ , with probability at least

$$1 - \exp\left(-\frac{2(N_m\eta_{m,\delta} - Q)^2}{N_m}\right) - 2d \exp\left(-\frac{Q\epsilon^2}{2L^2\delta^2}\right) - (1 - \eta_{m,\delta})^Q$$

the set  $A^{(u)}$  has  $|A^{(u)}| \geq Q$  elements, the inequality in (2) holds, and for at least one  $x_l^{(u)} \in A^{(u)}$  we have  $\|x_l^{(v)} - x^{(v)}\| \leq \delta$ . Since there are  $V$  modalities and the probability measures  $\nu_m^{(u)}$  are independent, with probability at least

$$1 - \left( \exp\left(-\frac{2(N_m\eta_{m,\delta} - Q)^2}{N_m}\right) + 2d \exp\left(-\frac{Q\epsilon^2}{2L^2\delta^2}\right) + (1 - \eta_{m,\delta})^Q \right)^V$$

there is at least one modality  $u \in \{1, \dots, V\}$  such that all of these three events occur. Now, let  $x_i^{(u)}, x_j^{(u)} \in B_\delta(x^{(u)})$  denote two training samples from this modality  $u$  and class  $m$ . As  $\|x_i^{(u)} - x_j^{(u)}\| \leq 2\delta$ , from the assumption (P2) on the embedding, we have  $\|y_i^{(u)} - y_j^{(u)}\| = \|f^{(u)}(x_i^{(u)}) - f^{(u)}(x_j^{(u)})\| \leq R_\delta$ . This gives

$$\begin{aligned} & \left\| f^{(u)}(x_i^{(u)}) - \frac{1}{|A^{(u)}|} \sum_{x_j^{(u)} \in A^{(u)}} f^{(u)}(x_j^{(u)}) \right\| \\ &= \left\| \frac{1}{|A^{(u)}|} \sum_{x_j^{(u)} \in A^{(u)}} (f^{(u)}(x_i^{(u)}) - f^{(u)}(x_j^{(u)})) \right\| \\ &\leq \frac{1}{|A^{(u)}|} \sum_{x_j^{(u)} \in A^{(u)}} \|f^{(u)}(x_i^{(u)}) - f^{(u)}(x_j^{(u)})\| \leq R_\delta. \end{aligned} \quad (20)$$

Then, for any  $x_i^{(u)} \in B_\delta(x^{(u)})$ , we have

$$\begin{aligned} & \|f^{(u)}(x^{(u)}) - f^{(u)}(x_i^{(u)})\| \\ &= \left\| f^{(u)}(x^{(u)}) - \frac{1}{|A^{(u)}|} \sum_{x_j^{(u)} \in A^{(u)}} f^{(u)}(x_j^{(u)}) \right. \\ &\quad \left. + \frac{1}{|A^{(u)}|} \sum_{x_j^{(u)} \in A^{(u)}} f^{(u)}(x_j^{(u)}) - f^{(u)}(x_i^{(u)}) \right\| \\ &\leq \left\| f^{(u)}(x^{(u)}) - \frac{1}{|A^{(u)}|} \sum_{x_j^{(u)} \in A^{(u)}} f^{(u)}(x_j^{(u)}) \right\| \\ &\quad + \left\| f^{(u)}(x_i^{(u)}) - \frac{1}{|A^{(u)}|} \sum_{x_j^{(u)} \in A^{(u)}} f^{(u)}(x_j^{(u)}) \right\| \\ &\leq L\delta + \sqrt{d}\epsilon + R_\delta \end{aligned} \quad (21)$$

where the last inequality follows from (2) and (20).

Now, through the training sample  $x_l^{(u)} \in B_\delta(x^{(u)})$  whose observation in modality  $v$  satisfies  $\|x_l^{(v)} - x^{(v)}\| \leq \delta$ , and from property (P1) of the embedding, we observe that the deviation between the embedding  $f^{(v)}(x^{(v)})$  of the observation  $x^{(v)}$  of the test sample used by the classification algorithm and the unknown embedding  $f^{(u)}(x^{(u)})$  of its unavailable observation  $x^{(u)}$  is bounded as

$$\begin{aligned} & \|f^{(v)}(x^{(v)}) - f^{(u)}(x^{(u)})\| \leq \|f^{(v)}(x^{(v)}) - f^{(v)}(x_l^{(v)})\| \\ & \quad + \|f^{(v)}(x_l^{(v)}) - f^{(u)}(x_l^{(u)})\| + \|f^{(u)}(x_l^{(u)}) - f^{(u)}(x^{(u)})\| \\ & \leq L\delta + \eta + L\delta = 2L\delta + \eta \end{aligned}$$

where the second inequality follows from the Lipschitz continuity of the interpolators  $f^{(v)}$  and  $f^{(u)}$ , and (P1). Combining this with (21), we get that for the training samples  $x_j^{(u)} \in A^{(u)}$

$$\begin{aligned} & \|f^{(v)}(x^{(v)}) - f^{(u)}(x_j^{(u)})\| \\ & \leq \|f^{(v)}(x^{(v)}) - f^{(u)}(x^{(u)})\| + \|f^{(u)}(x^{(u)}) - f^{(u)}(x_j^{(u)})\| \\ & \leq (2L\delta + \eta) + (L\delta + \sqrt{d}\epsilon + R_\delta) \\ & = 3L\delta + \sqrt{d}\epsilon + R_\delta + \eta. \end{aligned} \quad (22)$$

Next, let  $x_k^{(r)}$  be a training sample from another class than  $m$ , observed in any view  $r = 1, \dots, V$ . The distance between the embeddings of  $x_k^{(r)}$  and the test sample  $x^{(v)}$  is lower bounded as

$$\begin{aligned} & \|f^{(v)}(x^{(v)}) - f^{(r)}(x_k^{(r)})\| \geq \\ & \|f^{(u)}(x_j^{(u)}) - f^{(r)}(x_k^{(r)})\| - \|f^{(v)}(x^{(v)}) - f^{(u)}(x_j^{(u)})\| \\ & > \gamma - (3L\delta + \sqrt{d}\epsilon + R_\delta + \eta) \end{aligned} \quad (23)$$

where the last inequality is obtained from the property (P3) of the embedding and the inequality in (22). Using in (23) the assumption (3) on the embedding, we get

$$\|f^{(v)}(x^{(v)}) - f^{(r)}(x_k^{(r)})\| > 3L\delta + \sqrt{d}\epsilon + R_\delta + \eta. \quad (24)$$

We finally observe from the inequalities (22) and (24) that the embedding of any training sample  $x_k^{(r)}$  from another class than  $m$  has distance larger than  $3L\delta + \sqrt{d}\epsilon + R_\delta + \eta$  to the embedding  $f^{(v)}(x^{(v)})$  of the test sample  $x^{(v)}$ , whereas there

are at least  $Q$  samples from the same class as  $x^{(v)}$  within a distance of at most  $3L\delta + \sqrt{d}\epsilon + R_\delta + \eta$ . We conclude that the test sample  $x^{(v)}$  is then correctly classified via nearest neighbor classification through its embedding  $f^{(v)}(x^{(v)})$ .  $\square$

### Proof of Theorem 2

*Proof.* Recall from Lemma 1 that with probability at least

$$1 - \exp\left(-\frac{2(N_m\eta_{m,\delta} - Q)^2}{N_m}\right) - 2d \exp\left(-\frac{Q\epsilon^2}{2L^2\delta^2}\right) - (1 - \eta_{m,\delta})^Q$$

the embedding  $f^{(u)}(x^{(u)})$  of the query sample in modality  $u$  has  $|A^{(u)}| \geq Q$  neighboring training samples from the same class  $m$ , the inequality in (2) holds, and for at least one  $x_l^{(u)} \in A^{(u)}$  we have  $\|x_l^{(u)} - x^{(v)}\| \leq \delta$ . Assuming that all these three events have occurred and following the same steps as in the proof of Theorem 1, we conclude that there are at least  $Q$  samples  $x_j^{(u)} \in B_\delta(x^{(u)})$  such that

$$\|f^{(v)}(x^{(v)}) - f^{(u)}(x_j^{(u)})\| \leq 3L\delta + \sqrt{d}\epsilon + R_\delta + \eta \quad (25)$$

while the distance of the embedding of any training sample  $x_k^{(r)}$  from another class to  $f^{(v)}(x^{(v)})$  is lower bounded as

$$\|f^{(v)}(x^{(v)}) - f^{(r)}(x_k^{(r)})\| > 3L\delta + \sqrt{d}\epsilon + R_\delta + \eta. \quad (26)$$

This implies that the  $Q$  samples of smallest distance to the embedding  $f^{(v)}(x^{(v)})$  of the query sample are all from class  $m$ . Hence, for  $K \leq Q$ , the precision rate over the  $K$  nearest neighbors is

$$P = K/K = 1.$$

Similarly, when  $K > Q$ , at least  $Q$  of the  $K$  nearest neighbors of  $f^{(v)}(x^{(v)})$  are from the same class  $m$ , hence we get

$$P \geq Q/K.$$

Meanwhile, when  $K \leq Q$ , the retrieval algorithm returns  $K$  samples out of the  $N_m$  training samples from the same class  $m$ , hence

$$R = \frac{K}{N_m}.$$

Finally, when  $K > Q$ , since at least  $Q$  of the retrieved training samples will be from the same class as the query sample, we have

$$R \geq \frac{Q}{N_m}.$$

$\square$